Mission Performance of the GLAS Thermal Control System - 7 Years In Orbit

Eric W. Grob[1]
NASA Goddard Space Flight Center, Greenbelt, MD 20771

ICESat (Ice, Cloud and land Elevation Satellite) was launched in 2003 carrying a single science instrument – the Geoscience Laser Altimeter System (GLAS). Its primary mission was to measure polar ice thickness. The GLAS thermal control architecture utilized propylene Loop Heat Pipe (LHP) technology to provide selectable and stable temperature control for the lasers and other electronics over a widely varying mission thermal environment. To minimize expected degradation of the radiators, Optical Solar Reflectors (OSRs) were used for both LHP radiators to minimize degradation caused by UV exposure in the various spacecraft attitudes necessary throughout the mission. Developed as a Class C mission, with selective redundancy, the thermal architecture was single string, except for temperature sensors used for heater control during normal operations. Although originally planned for continuous laser operations over the nominal three year science mission, laser anomalies limited operations to discrete measurement campaigns repeated throughout the year. For trending of the science data, these periods were selected to occur at approximately the same time each year, which resulted in operations during similar attitudes and beta angles. Despite the laser life issues, the LHPs have operated nearly continuously over this time, being non-operational for only brief periods. Using mission telemetry, this paper looks at the performance of the thermal subsystem during these periods and provides an assessment of radiator degradation over the mission lifetime.

Nomenclature

AOI	=	Angle Of Incidence
CLHP	=	Component LHP
ESH	=	Equivalent Solar Hours
LHP	=	Loop Heat Pipe
LLHP	=	Laser LHP
MLI	=	Multi-Layer Insulation
PID	=	Proportional, Integral, Differential
PM	=	Primary Mirror
SM	=	Secondary Mirror
β	=	beta angle, the angle between the solar vector and orbit plane
α	=	Solar absorptance
ε	=	Infrared absorptance

[1] Staff Engineer, Thermal Engineering Branch, Applied Engineering Directorate, M/S 545, non-member.

I. Introduction

A key parameter used in the thermal design for satellites is the solar absorptance of the thermal radiator coating; especially for use in low earth orbits where direct or reflected sun is typically incident upon them. This parameter, along with the IR absorptance ("emissivity") and internal heat generation, establishes the thermal balance of the satellite or instrument in the mission thermal environments. Design conservatism dictates that this value adequately accounts for degradation due to on-orbit effects and contamination to ensure thermal control is maintained over the mission lifetime. During the development phase, much effort goes into calculating the estimated degradation of these surfaces, and measured BOL and expected EOL values are applied to bound the thermal design cases. This degradation over time is not linear between these values; rather it follows an exponential curve, with an initial increase in solar absorptance during the early mission due to material outgassing, and tapering off after the first few months of the mission. Unfortunately, there is usually no assessment during or after the operational lifetime, due to funding constraints, to verify the accuracy of these degradation estimates. A recent opportunity for a NASA Goddard Space Flight Center mission allows this verification to be made.

Figure 1. ICESat w/GLAS Instrument.

Launched in 2003, ICESAT flies in a 600 kilometer, 94° inclined, non-synchronous orbit that results in a large beta angle range over the mission life. At this altitude, there is an eclipse most of the time, except when the beta angle increases above 67°. The solar arrays have a single axis of rotation (Figure 1), so to maintain sufficient illumination in the higher beta angles, the spacecraft yaws at +/-33° beta. This places the spacecraft in two distinct orientations: "sailboat" for $33° < |\beta| < 90°$ and "airplane" when $0° < |\beta| < 33°$. With the LLHP radiator and CLHP radiators facing +Y and -Y, respectively, the yaw rotations were selected to keep the Laser LHP radiator (+Y) in the coldest and most stable environment and a yaw at $\beta = 0°$ was added.

The primary thermal design requirement for GLAS was to provide a thermally stable optical bench to minimize distortion of the outgoing beam path and the receive telescope. The driving requirement was maintaining the lasers with better than 0.3°C/5 minute stability. Shortly after launch and activation, an early assessment (Reference 1) showed the thermal control met these challenging requirements.

This was especially challenging in the widely varying thermal environment - Figure 2 illustrates the orbit average flux versus beta angle for each radiator, with the respective hot and cold cases identified. These requirements were achieved by using Loop Heat Pipe (LHP) technology to eliminate the variations of the external environment, due to diurnal/seasonal effects, yaw maneuvers and mission degradation.

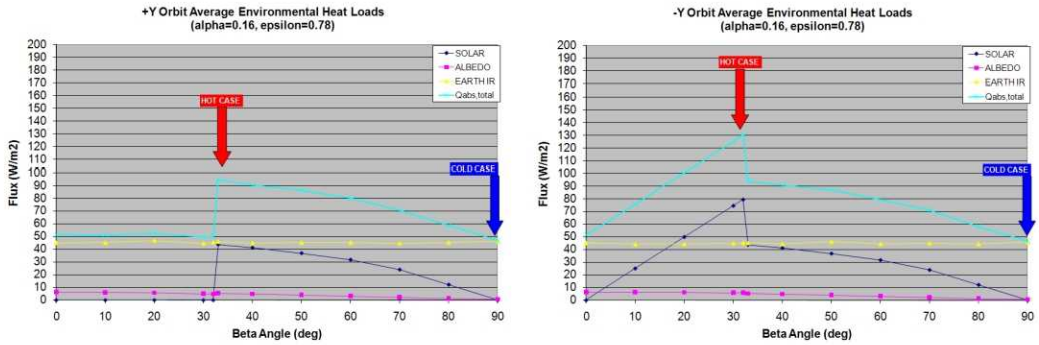

Figure 2. GLAS LHP Radiator Environmental Heating.

The GLAS instrument design is based on two perpendicular benches: the Main Optical Bench (MOB) and the Telescope Deck (TD). The MOB is a two-sided optical bench, with aluminum facesheets and honeycomb core. The lasers are mounted on one side and the housekeeping electronics and navigation equipment on the other. The TD mounts the telescope looking earthward to gather the return optical signal, along with the receive optics and detectors.

The GLAS thermal control architecture uses a network of Constant Conductance Heat Pipes (CCHPs) to link these distributed components to the LHPs, with the 3 lasers linked to a dedicated Laser LHP and the other avionics

linked to the Component LHP. Appendix I shows a schematic diagram of the GLAS thermal control subsystem and the thermal models used during the development phase. Electronic heater controllers are used for adjustable LHP, telescope, and Etalon Filter setpoint control. Survival heater control is provided by mechanical thermostats and has rarely been needed since launch.

II. Discussion of Operational Cases Assessed

As designed, the GLAS LHPs maintain a constant evaporator temperature in the widely varying external environment. This is achieved by sizing the radiator to provide sufficient condenser tubing length (radiator area) to ensure full condensing of the vapor and an additional length to subcool the liquid before returning to the compensation chamber. Accurate fluid inventory and system design allow the LHPs to perform as expected, otherwise, operational issues could develop (Reference 2). For a given heat load and setpoint temperature, in a steady external environment the length of the radiator condensing section is constant, but in a varying environment, the length increases and decreases as the environment increases and decreases. With a constant heat load from the electronics into the evaporator, the temperature of the liquid returning from the radiator varies based on the changing absorbed environmental heat load – as the environment increases, additional length is required to fully condense the vapor leaving less length for subcooling. With the same temperature control setpoint and external environment, radiator degradation would result in a gradual increase in the condenser length, and in the temperature of the returning liquid.

For GLAS, the environmental variation would include the eclipse and beta angle variations, plus any long term radiator degradation effects. As an optical instrument, stringent cleanliness was enforced throughout the development and assembly phase, so outgassing contamination was expected to be minimal. The eclipse effects would have a diurnal profile as the satellite orbits the Earth through sunlight then eclipse, and also a seasonal profile due to the changing beta (and yaw) angle.

A longer term upward trend would be due to an increased solar absorptance, indicative of radiator degradation, so environments with higher solar incidence should provide the best indication of degradation. Solar exposure estimates have been previously calculated for the two LHP radiators showing ~5300 ESH and ~7300 ESH for the +Y and –Y radiators, respectively over the seven years of operations. The periodic yaw rotations result in higher solar exposure to the –Y LHP radiator in the $-32° < \beta < +32°$ range (Figure 2) with the maximum near $|\beta| < +32°$ just after the yaw maneuver to airplane mode. The +Y radiator, as designed, gets much less solar exposure, so degradation would be expected to be less and less easily detected due to the lower solar exposure, with its "peak" at $|\beta| < +32°$ just before the yaw to airplane mode. During the design phase, Optical Solar Reflectors (OSRs) were selected for the GLAS radiators (Figure 3) to a low initial solar absorptance and to minimize degradation due to solar exposure typically seen with other coatings, such as silver Teflon or paints.

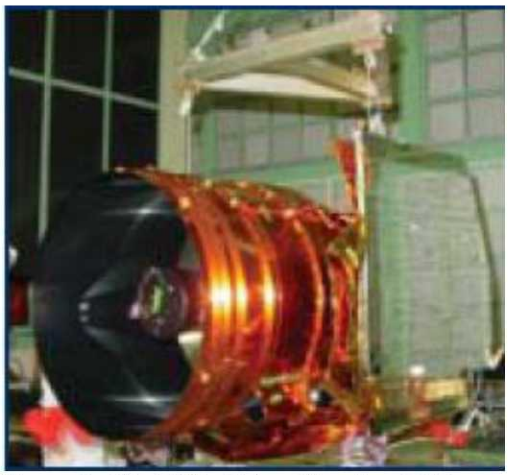

Figure 3. GLAS Radiator Showing OSRs.

Since the orbit environments are very different for these two satellite orientations, a comparison can only be made between cases in similar orientations. To assess the liquid temperature returning from the radiator, telemetry from operational periods having similar beta angles would minimize the seasonal beta angle effect. Four telemetry points are available for each of the two LHPs, but the temperature of the liquid returning from the radiator is the key to determining radiator degradation.

TGLLHPxEVAPT	LHP Evaporator Temperature (on end of evaporator near vapor line exit)
TGLLHPxLLCCT	LHP Liquid Line Temperature (at compensation chamber)
TGLLHPxRADT	**LHP Liquid Temperature (at liquid line exit from radiator)**
TGLLHPxVLT	LHP Vapor Line Temperature (before entering radiator)

These telemetry mnemonics would include x=1 for the Laser (+Y) LHP and x=2 for the Component (-Y) LHP.

Although the original mission operation plan was for constant laser operations, switching lasers only as they

degraded after a period of about 18 months, design flaws within the lasers caused the first laser to fail after only 31 days of operation. Investigation into the cause of this failure led to a revised operations plan with laser firing for ~30 days periods only a few times per year. This operations approach prolonged the mission, with the lasers lasting for nearly seven years. For science data comparison, these periods were aligned at the same time of year throughout the mission. Figure 4 illustrates this intermittent operation alongside the beta and yaw angle variations.

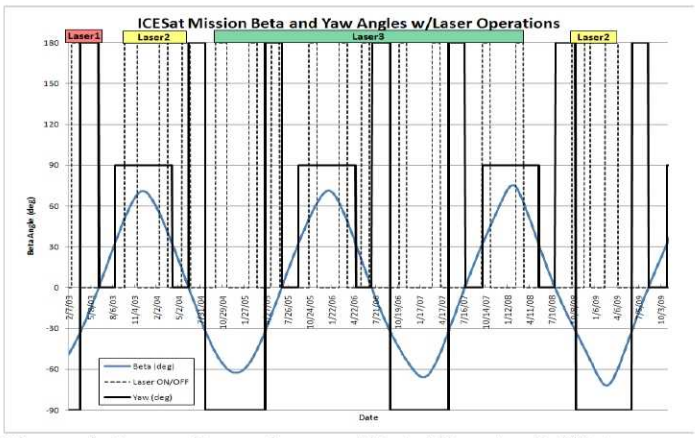

Figure 4. Laser Operations and Beta/Yaw Angle History.

From a thermal correlation perspective, being able to compare the first operational period to several others over the mission lifetime would provide the best trending of radiator degradation. Table 1 summarizes beta angle ranges and LHP setpoints for all seventeen operational campaigns in chronological order through 2009 showing that thirteen of the cases were in the high beta range ($|\beta| > 33°$) and four in the low beta range ($|\beta| < 33°$). By "binning" the cases into 10° beta angle bands and highlighting those with the same setpoints within those bands, the cases to be compared in detail becomes evident. Although numerous cases have the same setpoint, they don't always occur in the same beta angle range, so comparing them in detail introduces the incident flux as another variable. Since this is not a correlation using a thermal model, detailed comparisons will only be made for "identical" scenarios; L3A, L3B, L3H for CLHP and L3C, L3F for LLHP.

Table 1. ICESat Mission Instrument Operational Periods.

Campaign (L#)	Start	Stop	# days	Beta Angle(°) Start	Stop	Mean	LLHP Tset °C Start	Stop	CLHP Tset °C Start	Stop	Operational Periods Occuring Over Beta Angle Range 0-10	10-20	20-30	30-40	40-50	50-60	60-70	70-80	80-90
L1	02/19/03	03/26/03	35	-45.0	-32.8	38.9	19.4	12.4	17.6	17.6				Y					
L2a	09/24/03	11/17/03	54	50.7	68.9	59.8	16.0	16.0	10.7	16.6						Y			
L2b	02/16/04	03/20/04	33	53.8	40.1	46.9	16.0	16.0	16.6	16.6					Y				
L2c	05/17/04	06/20/04	34	12.9	-3.7	4.6	16.0	5.9	6.6	6.6	Y								
L3a	10/02/04	11/07/04	36	-48.1	-57.6	52.8	**6.0**	**8.2**	**14.1**	**14.1**						Y			
L3b	02/16/05	03/23/05	35	-55.6	-44.6	50.1	8.2	8.2	**14.1**	**14.1**						Y			
L3c	05/19/05	06/22/05	34	-20.0	-3.6	11.8	**6.0**	**6.0**	6.1	6.1		Y							
L3d	10/20/05	11/23/05	34	50.6	62.6	56.6	**6.0**	**6.0**	13.1	13.1						Y			
L3e	02/21/06	03/27/06	34	62.2	48.0	55.1	**6.0**	**6.0**	15.0	15.0						Y			
L3f	05/23/06	06/25/06	33	20.2	4.0	12.1	**6.0**	**6.0**	8.0	8.0		Y							
L3g	10/24/06	11/26/06	33	-44.4	-54.0	49.2	6.0	6.0	13.1	13.1					Y				
L3h	03/11/07	04/13/07	33	-59.4	-46.9	53.2	**6.0**	**6.0**	**14.1**	**14.1**						Y			
L3i	10/01/07	11/04/07	34	32.0	45.8	38.9	6.0	6.0	14.3	14.3				Y					
L3j	02/16/08	03/20/08	33	74.0	61.5	67.8	6.0	6.0	15.0	15.0							Y		
L3k	10/03/08	10/18/08	15	-27.0	-32.0	29.5	**6.0**	**6.0**	10.1	10.1			Y						
L2d	11/24/08	12/16/08	22	-45.0	-53.0	49.0	6.0	11.0	14.1	14.1					Y				
L2e	02/16/09	04/10/09	53	-70.0	-59.0	64.5	11.0	13.0	14.1	14.1							Y		
L# = Laser #	17									Qty:	1	2	1	2	3	6	2	0	0

LHP telemetry for the Component and the Laser LHPs, along with the beta angle ($|\beta|$), is shown for all operational cases in Appendix II. From these plots, the effect of the changing environment can be seen on the return liquid temperature, giving higher diurnal oscillations in the lower part of the high beta range where both LHP radiators "flip" through the sun. Similarly, larger oscillations can be seen for the CLHP in the higher part of the low beta range where the sun is more directly incident on its radiator, and the LLHP radiator is out of direct sun, although the albedo flux onto it does increase as the beta angle decreases. In the lower beta range ("sailboat" mode) cases, the CLHP radiator is towards the sun with an AOI of 0° to 32°, while the LLHP radiator is out of direct sun. In

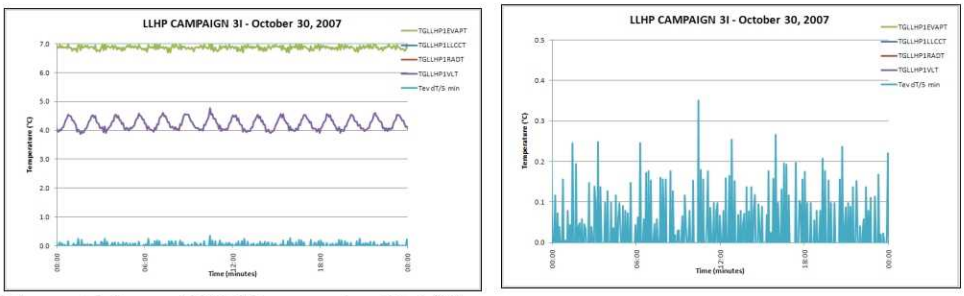

Figure 5. Laser LHP Evaporator Stability.

the very high beta range, these oscillations are small due to the small angle of incidence of the sun on the radiators. The telemetry reflects this in the larger oscillations on the CLHP return liquid temperature.

Figure 5 shows the evaporator temperature of the Laser LHP over a 24 hour period in its worst case transient thermal environment, showing <0.3°C stability at the evaporator which yields <0.2°C/5 minutes at the Laser itself due to its thermal mass.

III. Assessment of Loop Heat Pipe Radiator Degradation

Degradation is expected to be most apparent in the low beta range on CLHP, due to higher solar flux and increased AOI. Detailed plots of the liquid return temperature for representative 24 hour periods in all operational cases is shown in Appendix 3 for CLHP and Appendix 4 for LLHP. Unfortunately, these periods used different CLHP setpoints and the data isn't easily assessed without the use of a thermal model, but cases 3c and 3f can be assessed for LLHP. In the high beta range, the same criteria allows a detailed assessment of 3a, 3b, and 3h (CLHP) and 3a, 3d, 3e, and 3h (LLHP).

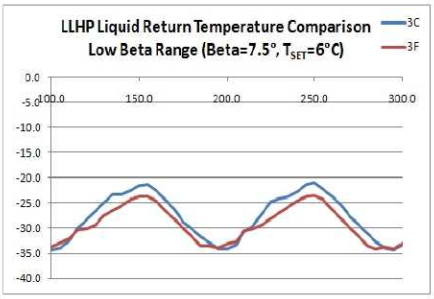

Figure 6 - LLHP Low Beta Comparison

Data for the LLHP in cases 3c and 3f match very closely, although the peak and average temperatures appear warmer for 3c. This is confirmed in Figure 6 showing two orbit close-ups (β=7.5° and T_{SET}=6°C), with their peaks aligned [for illustrative purposes only]. The larger than expected difference of peak (daylight) temperatures >3°C between them is apparent, suggesting increased heating on the radiator versus higher dissipation, which would manifest itself by a higher average temperature as well. Since 3c occurred before 3f, neither laser degradation (higher dissipation) or degradation (higher absorptance) can be the cause – it is likely the local albedo of the earth in these two particular 3c orbits is higher than the 3f orbits compared.

In the high beta range (Figure 7), for CLHP, the data is very similar for all three periods and aligning the peaks shows only a 0.5°C difference in temperatures between the data. For LLHP, the data also shows very consistent data for the four periods assessed with peaks within 0.7°C of each other.

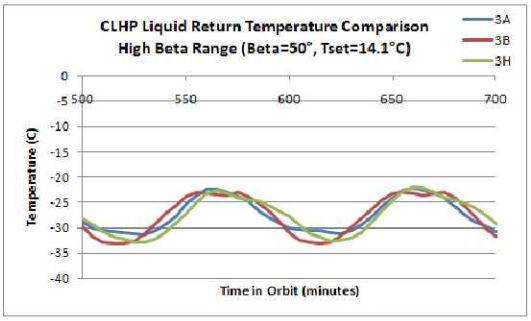

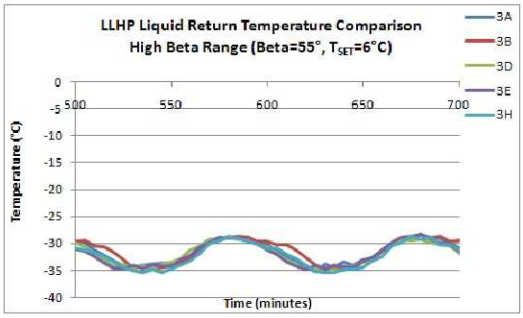

Figure 7. CLHP and LLHP High Beta Detailed Comparison.

IV. Assessment of Telescope Thermal Control

The GLAS telescope consists of the primary and secondary mirrors, supported by the light baffle tower. The telescope is shielded from direct sunlight by the circular sunshade whose height extends beyond the secondary mirror sufficiently to prevent direct sunlight from impinging on the SM at any point in the orbit over the entire beta range. Temperature control is provided by heater circuits on the primary mirror, secondary mirror, and baffle. All are PID control with adjustable setpoints from 0° to 30°. The secondary mirror and baffle tower are insulated with MLI. There are no dedicated radiators for telescope - the primary mirror acts as the only "radiator" looking to earth at all times. The Etalon filter is used to tune the bandwidth of the return signal filter to two different temperatures for the lasers. These temperatures were specified during the development phase as 29° and 42°C.

Three telemetry points are available for the telescope and a single point for the Etalon:

GHKPMIRT	Primary Mirror Temperature
GHKTOWT	Baffle Tower Temperature

GHKSMIRT	Secondary Mirror Temperature
GHKETTT	Etalon Filter Temperature

Temperature telemetry for the telescope and etalon filter, through all seventeen campaigns, is shown in Appendix 5. At a high level, the data shows stable temperature control through the operational periods. A more detailed assessment, however, shows the effect of the environment on the telescope in the low beta range where sunlight and albedo enter the sunshade opening, affecting the telescope temperature stability. Besides the repetitive orbit effects, a lower frequency effect is also noted in the lower beta range as well, resulting from the variation in albedo over the changing earth geography each orbit. Since the orbit is 95 minutes, the earth rotates ~23.5° under the orbiting satellite every orbit. This results in differing land/water/ice features every orbit and results in changing albedo effects from the local geography for a particular orbit.

This effect is shown to diminish as the beta angle increases (Figure 8); eventually the sunlight and albedo contribution is blocked, so the telescope thermal control is much more stable.

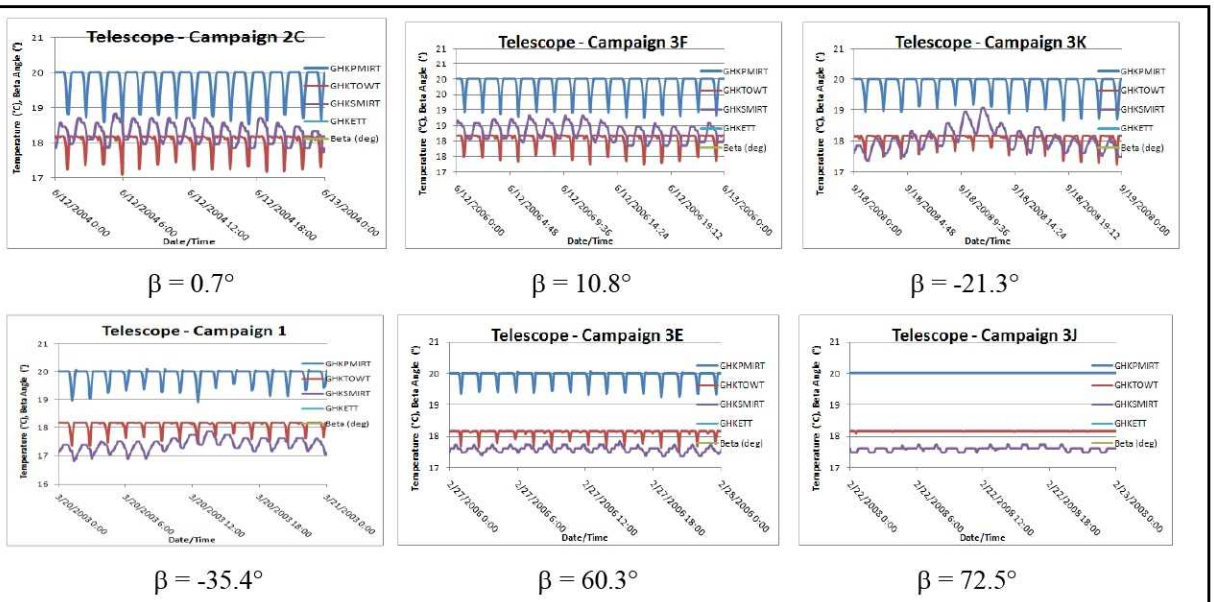

Figure 8 - Detailed Telescope Telemetry (In Order of Decreasing Beta Angle)

Thermal control of the Etalon Filter is shown to be very tightly controlled in all operational cases. Figure 9 highlights the stringent control in the most varying low beta thermal environment showing <0.05°C control.

V. Conclusion

Although understanding the degradation of thermal control coatings is critical to the design of all satellites, the lack of funding for an assessment at the end of a mission prevents this from being a regular activity. This study offers a unique assessment using flight data over a seven year mission period to provide a quantitative look at the GLAS thermal control subsystem performance, including degradation effects on the LHP radiators. Temperature control of the lasers and other avionics linked to the LHPs was shown to be stable in the widely varying mission thermal environments encountered over the mission lifetime. While this assessment finds little or no degradation for the part of the mission that could be assessed (L+20 thru L+92 months), most of the expected degradation would have occurred shortly after launch from initial outgassing of the satellite. An analytical assessment

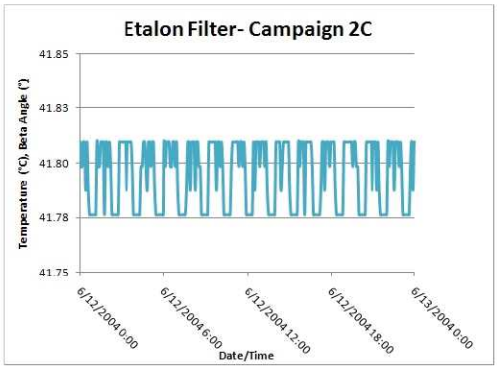

Figure 9 - Etalon Filter Temperature Stability

that can account for the different setpoints and thermal environments, using the L1 and early L2 data, may provide an indication of radiator coating degradation during the early mission operations. Subsequent degradation due to environmental effects was expected to be low for OSRs and this assessment verifies that conclusion. Thermal control of the telescope was shown to meet the requirements of the mission over the large range of external thermal environments and the precision control of the Etalon Filter over its large design range was demonstrated.

Acknowledgments

The author gratefully acknowledges Peggy Jester, Wallops Flight Facility, and the mission operations staff at the Laboratory for Atmospheric and Space Physics, for providing the mission data and for their efforts in operating GLAS over the mission.

References

[1]Grob, E., Baker, C., McCarthy, T., "In-Flight Thermal Performance of the Geoscience Laser Altimeter Syastem (GLAS) Instrument", *ICES International Conference on Environmental Systems,* Vancouver, BC, 2003, 2003-01-2421

[2]Grob, E., Baker, C., McCarthy, T., "Geoscience Laser Altimeter System (GLAS) Loop Heat Pipes-An Eventful First Year On-Orbit", *ICES International Conference on Environmental Systems,* Colorado Springs, CO, 2004, 2004-01-2558.

Appendix 1 - GLAS Thermal Control Architecture and Thermal Models

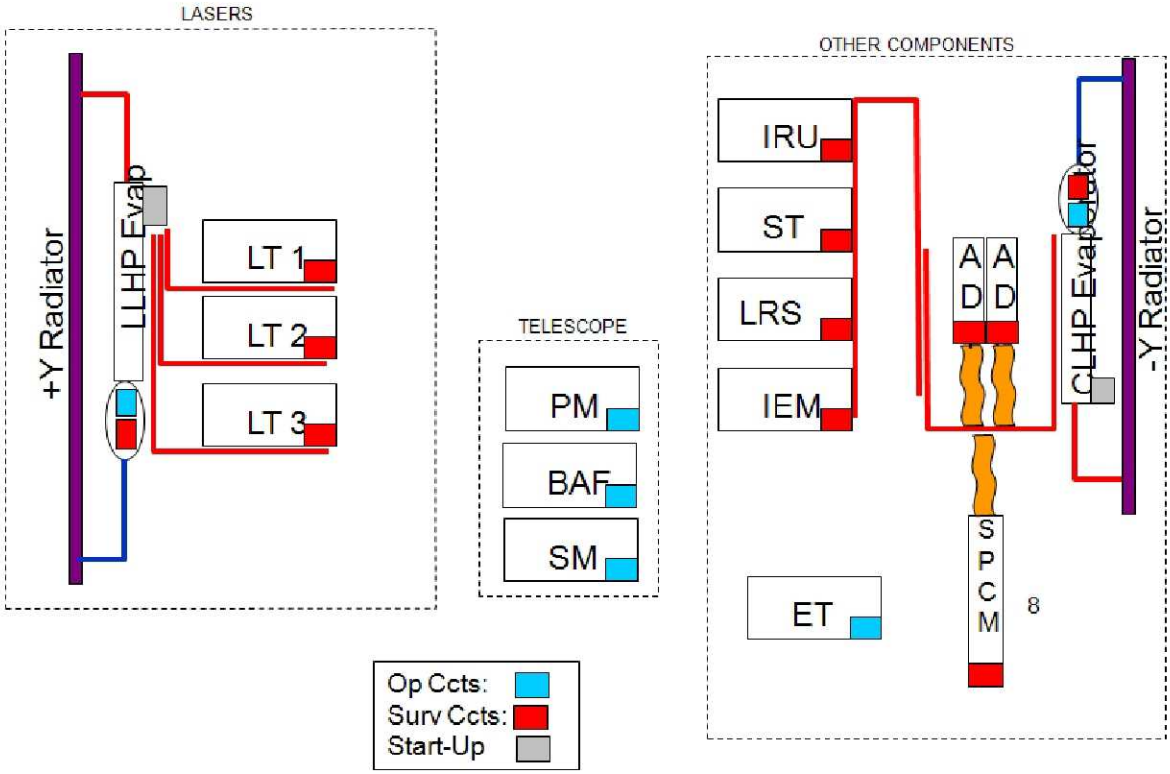

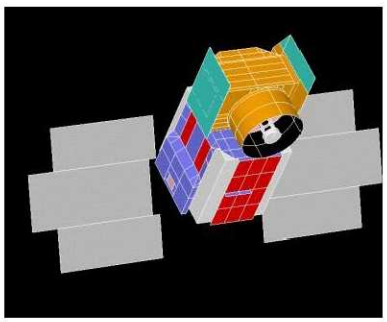

a) ICESat Geometric Model

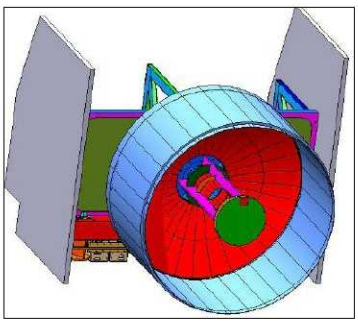

b) GLAS Geometric Model

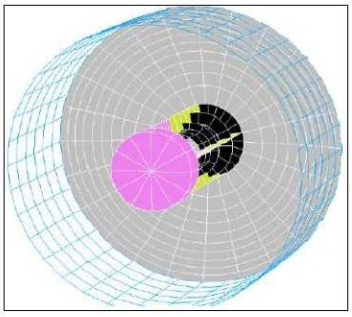

c) Telescope Geometric Model

Appendix 2 - LHP Telemetry Operational Cases

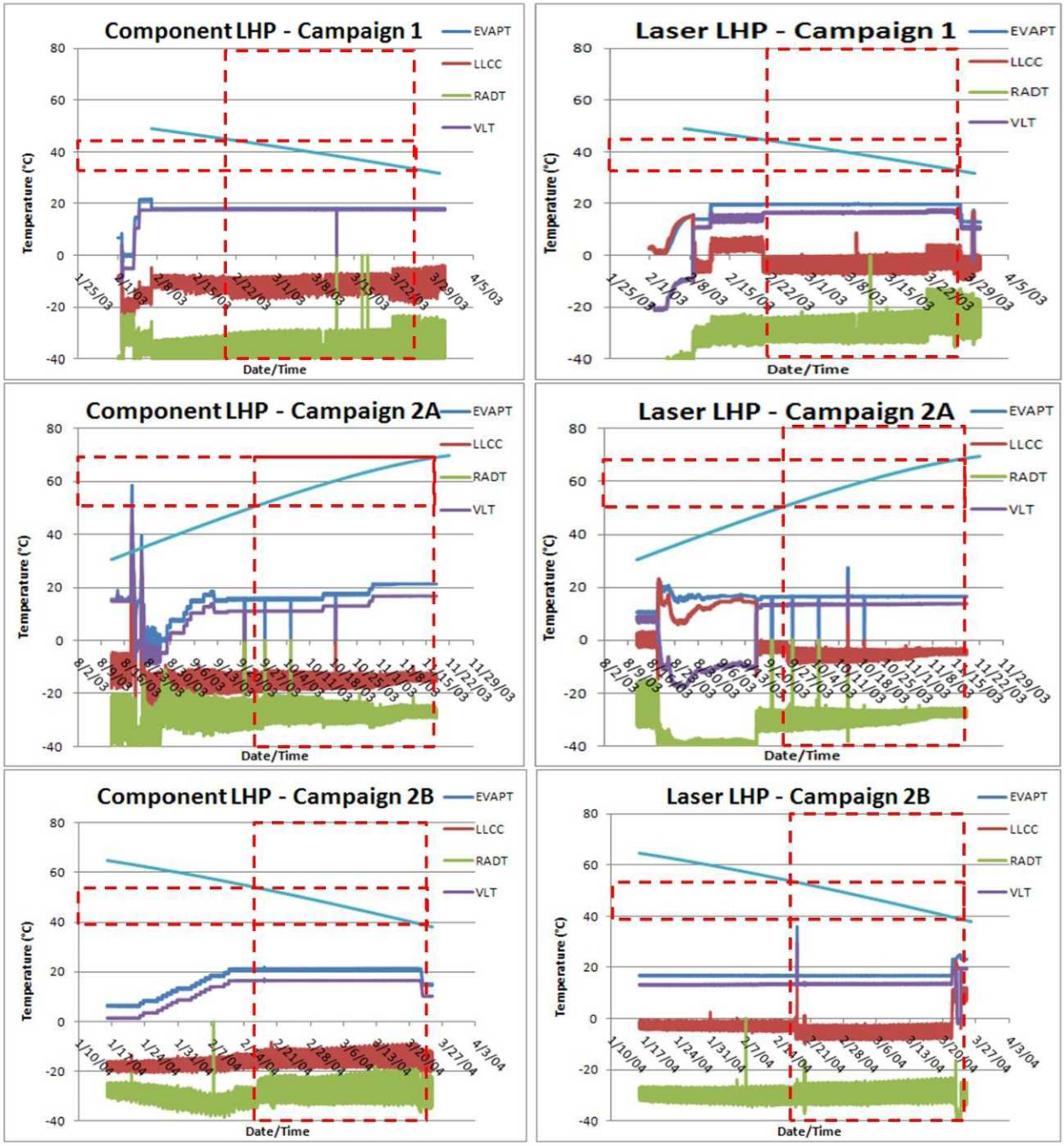

Appendix 2 - LHP Telemetry Operational Cases (continued)

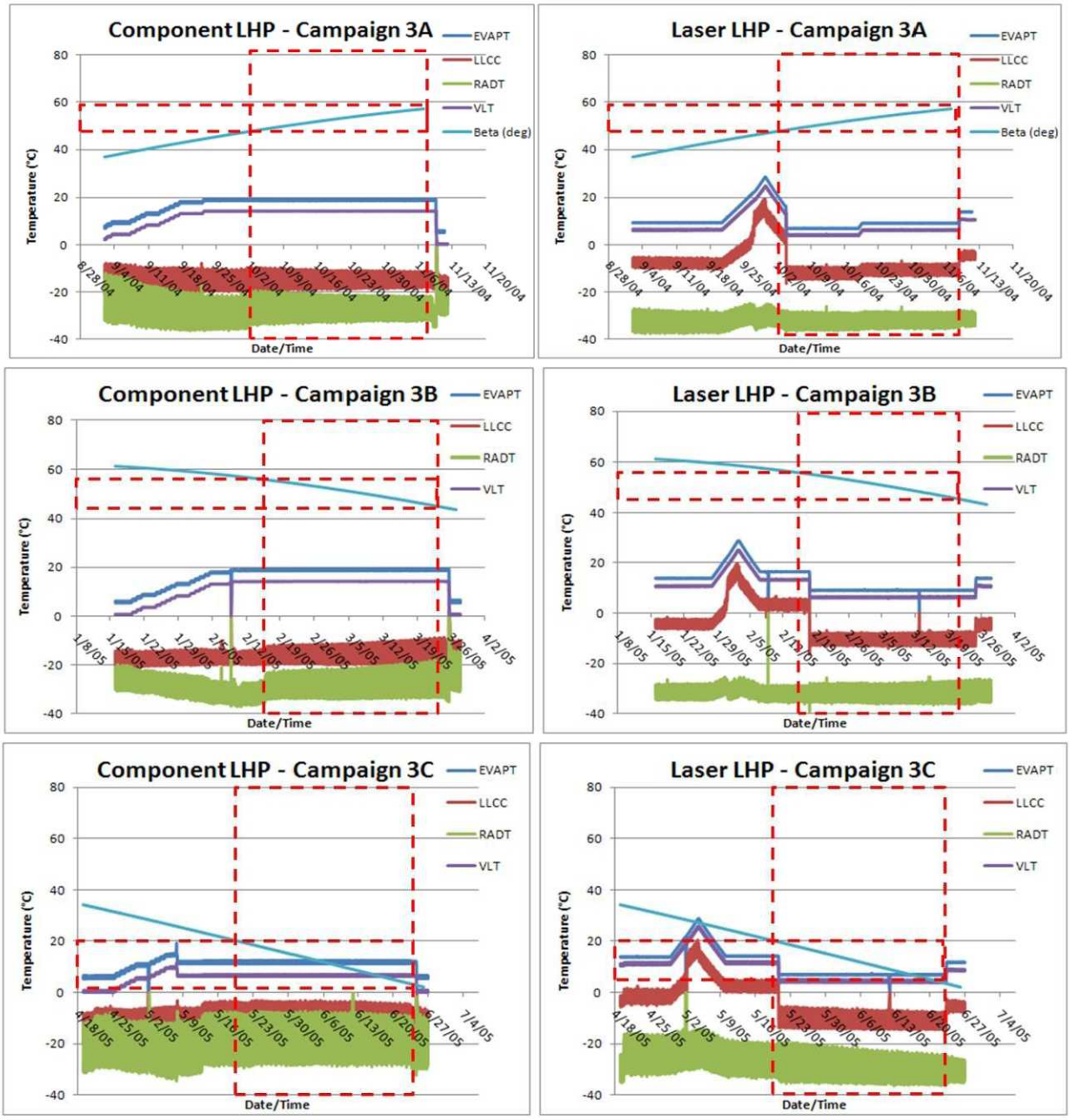

Appendix 2 - LHP Telemetry Operational Cases (continued)

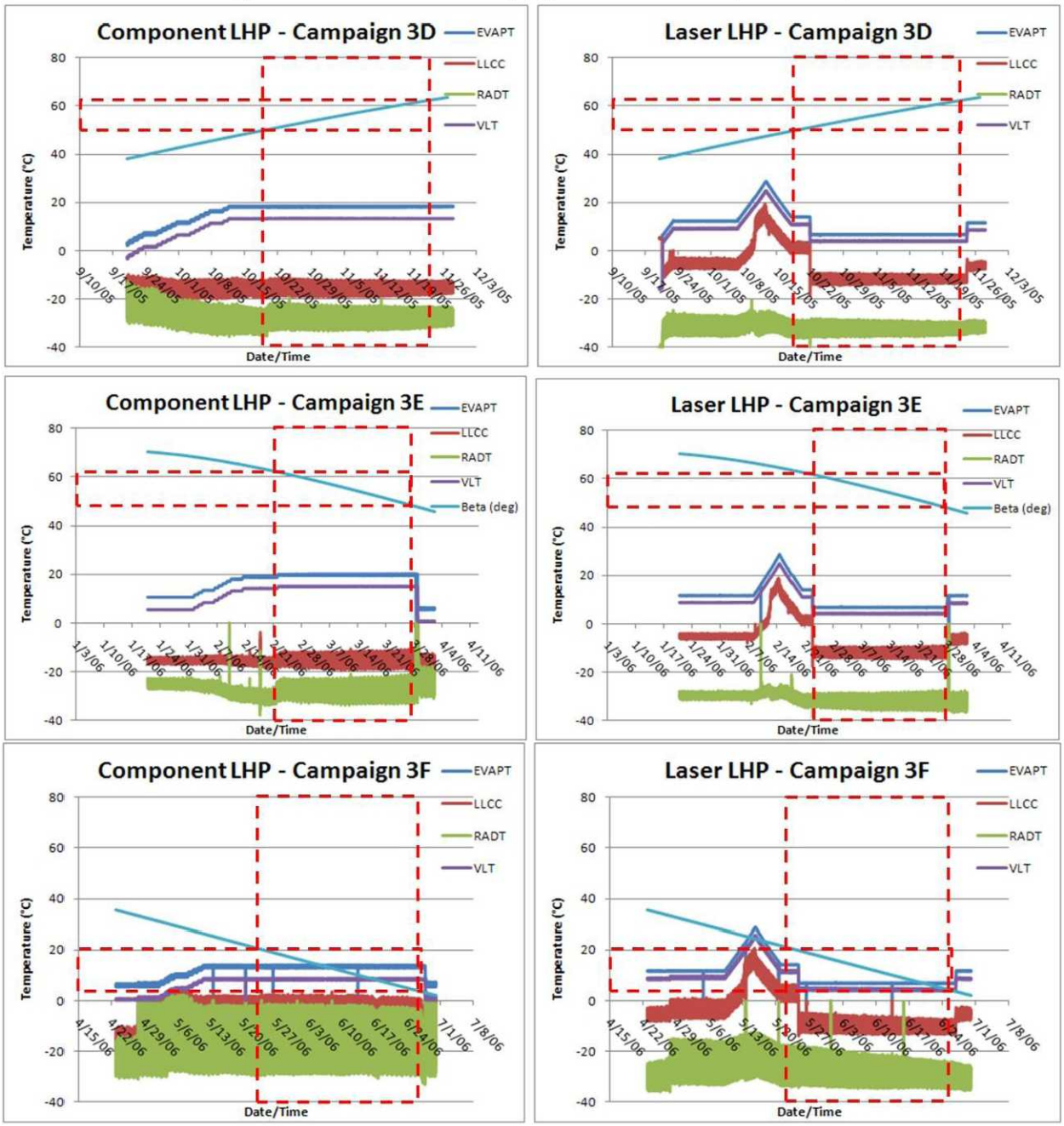

Appendix 2 - LHP Telemetry Operational Cases (continued)

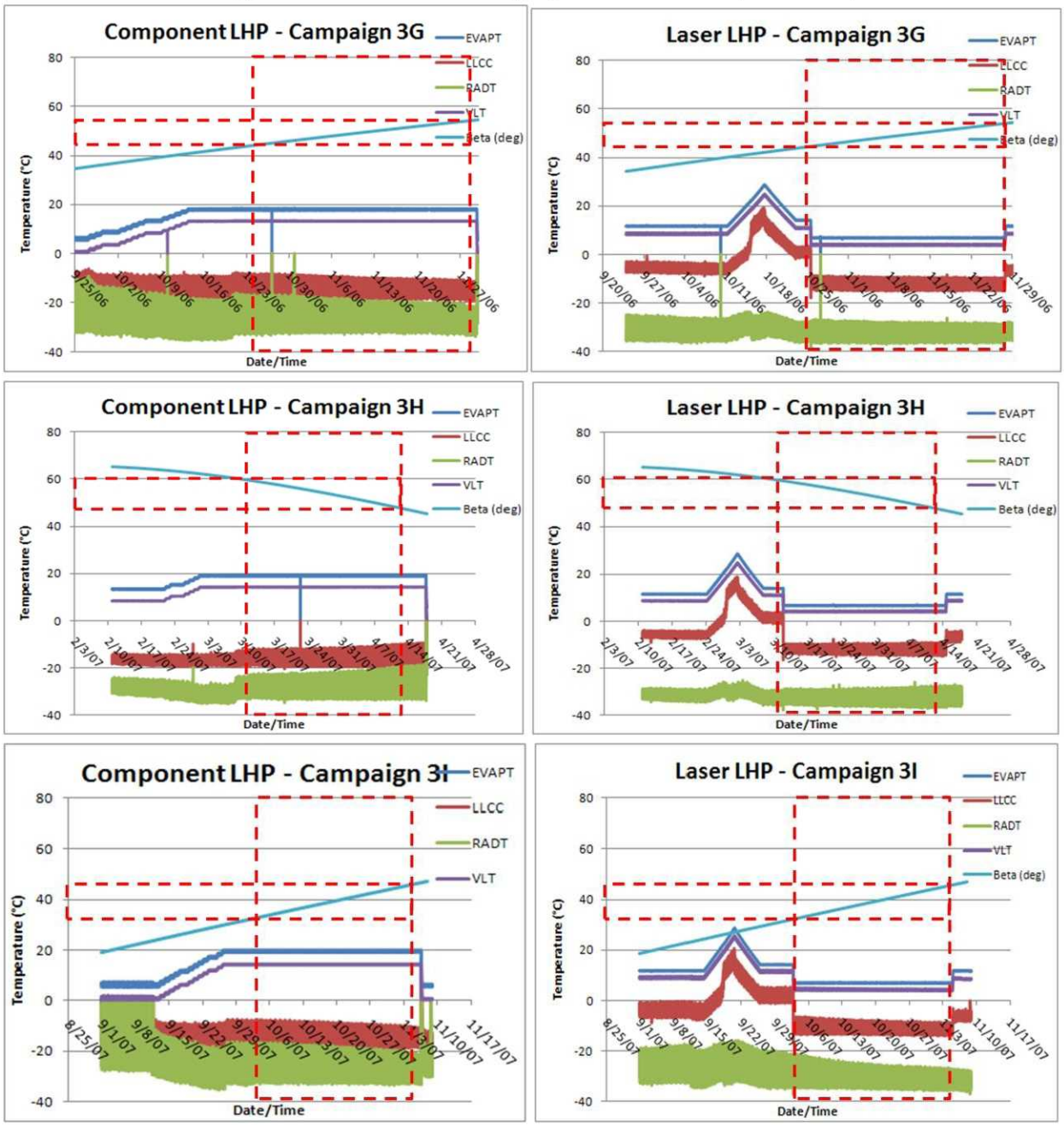

Appendix 2 - LHP Telemetry Operational Cases (continued)

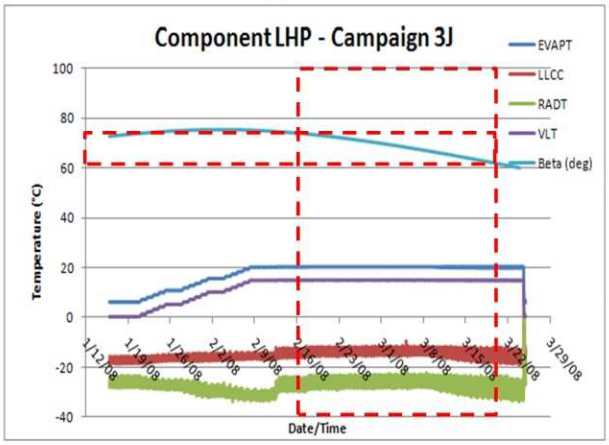

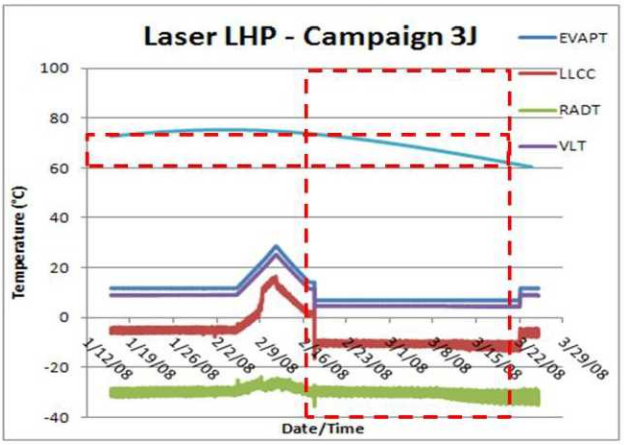

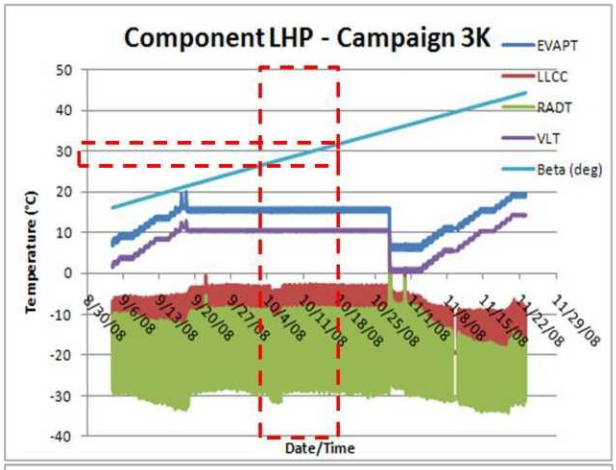

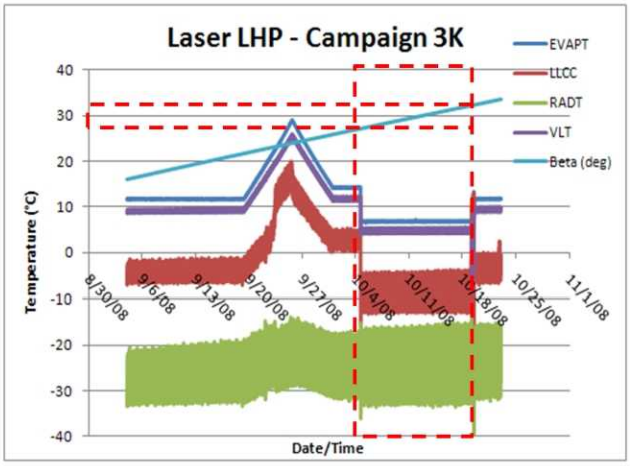

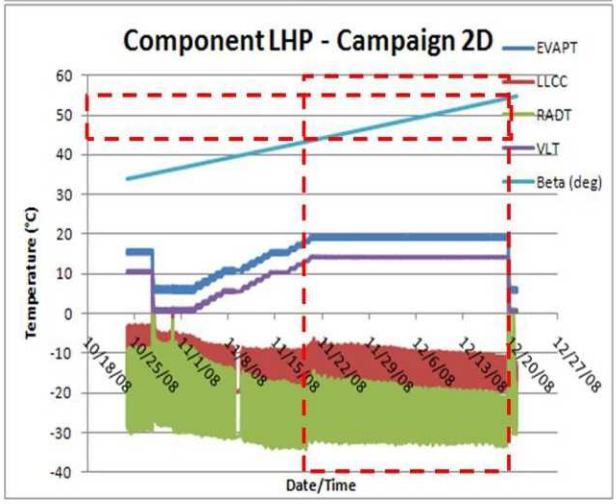

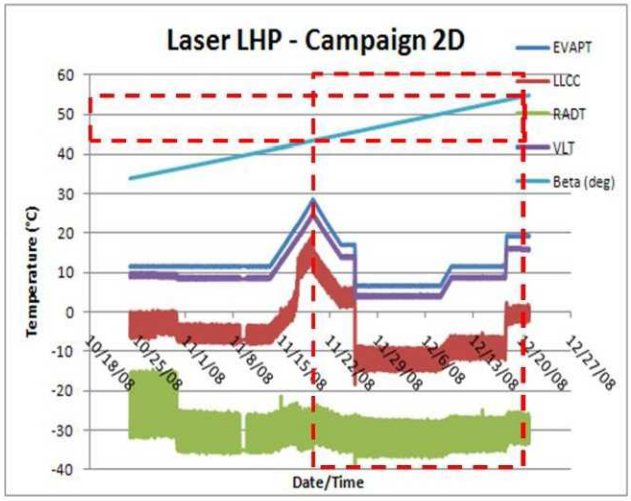

Appendix 2 - LHP Telemetry Operational Cases (continued)

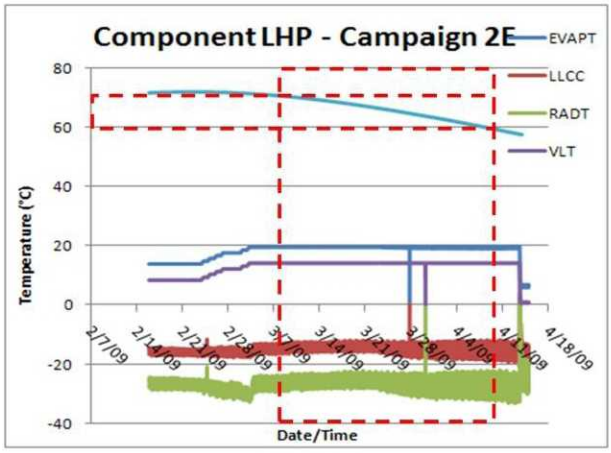

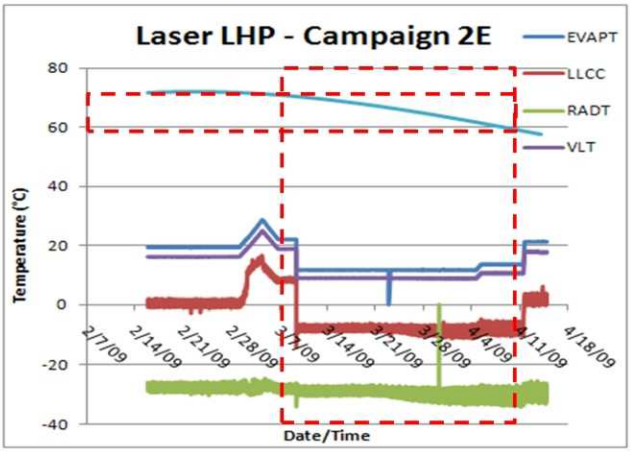

Appendix 3 - Detailed CLHP Liquid Line Temperatures

Low Beta Range (β=22°)

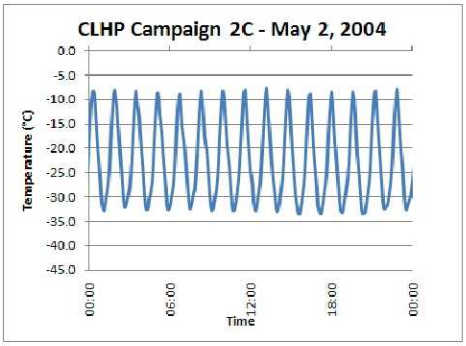

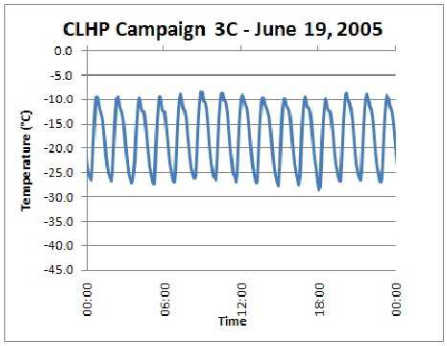

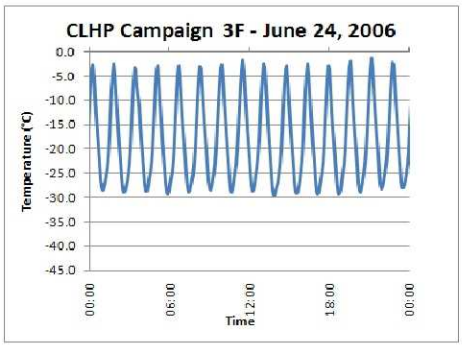

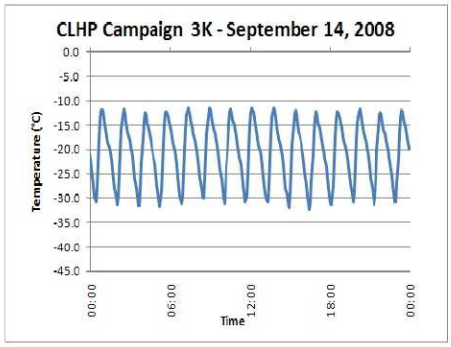

High Beta Range (β=50°)

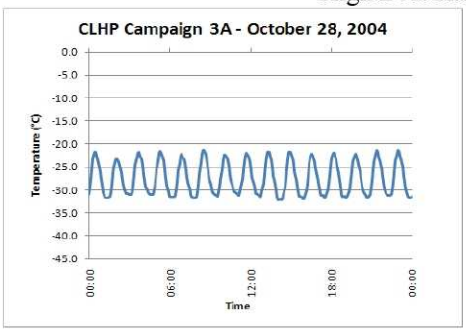

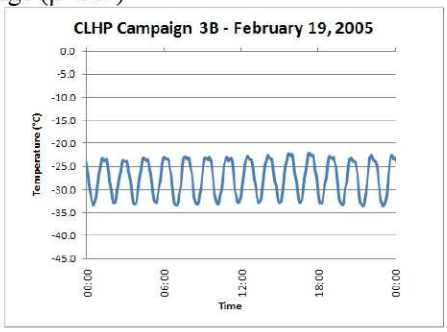

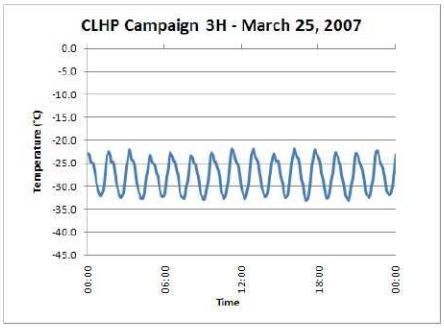

Appendix 4 - Detailed LLHP Liquid Line Temperatures

Low Beta Range (β=7.5°)

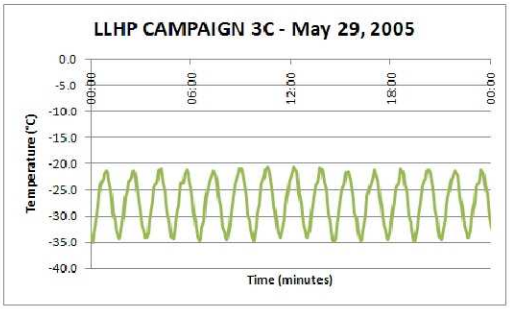

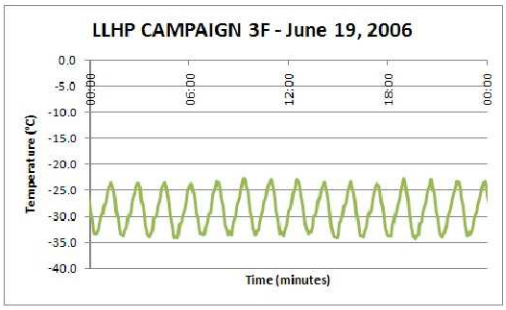

High Beta Range (β=55°)

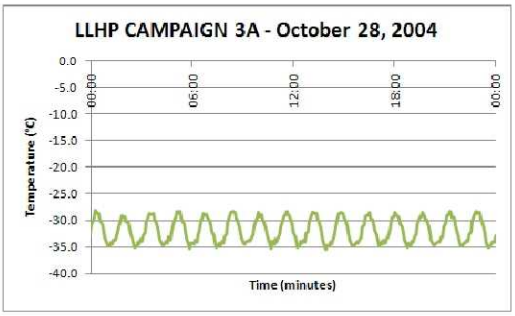

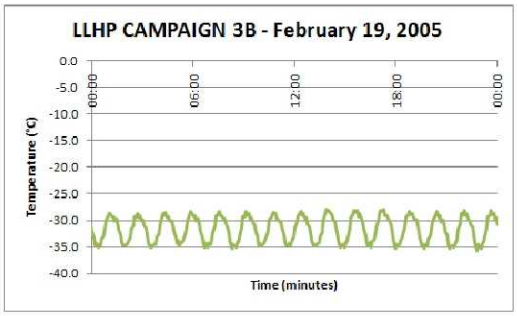

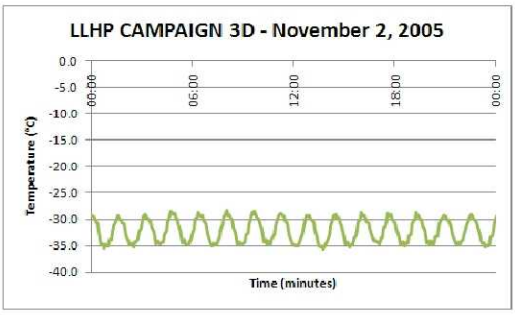

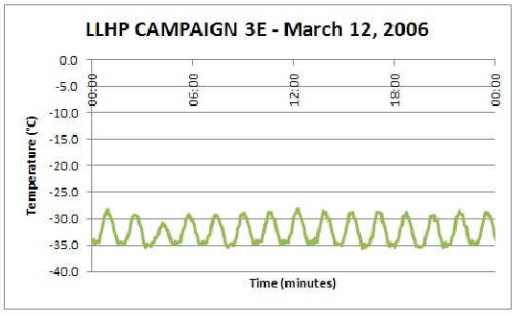

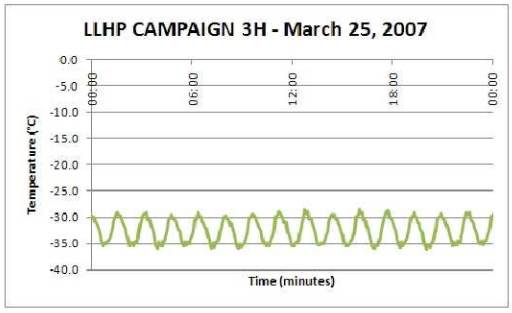

Appendix 5 - Telescope Telemetry

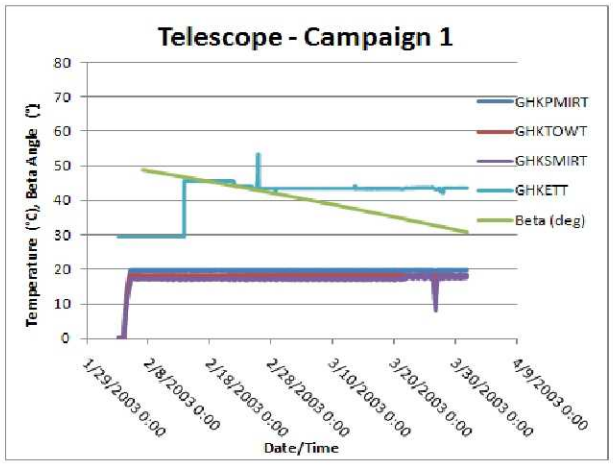

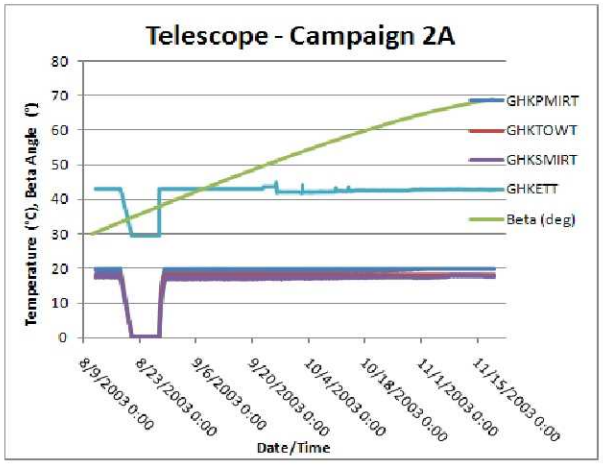

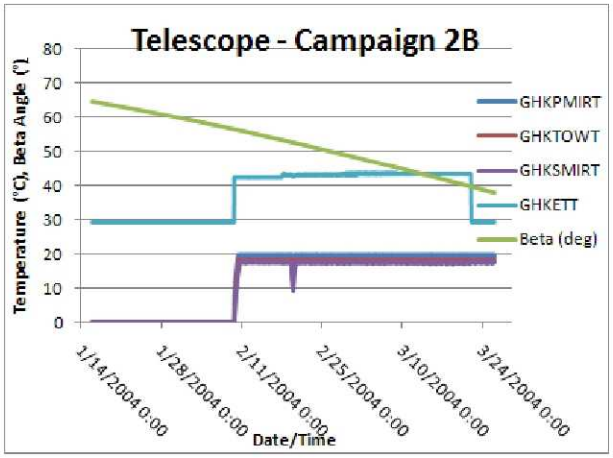

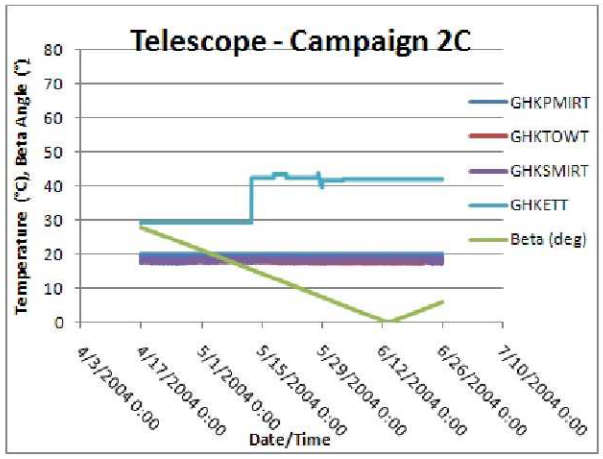

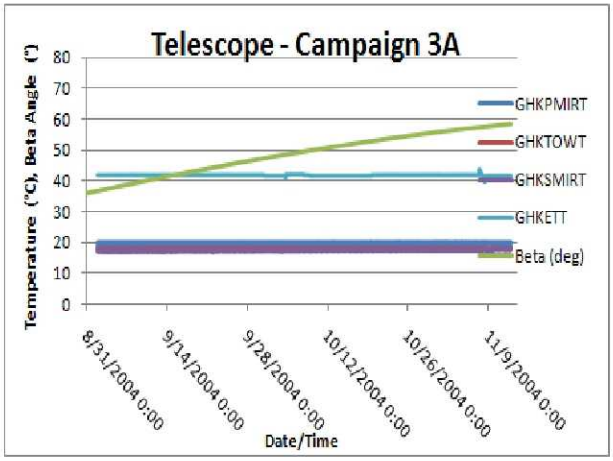

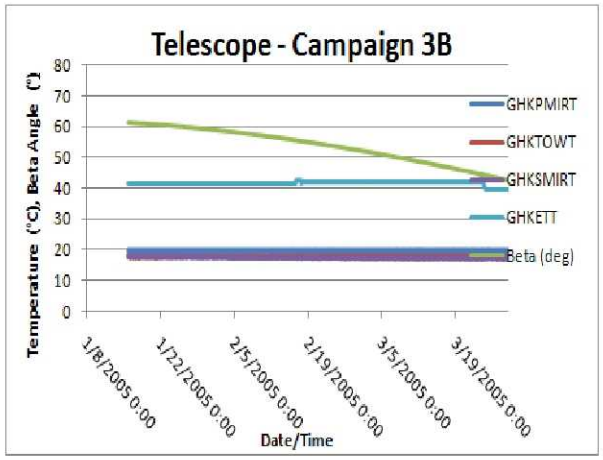

Appendix 5 - Telescope Telemetry (continued)

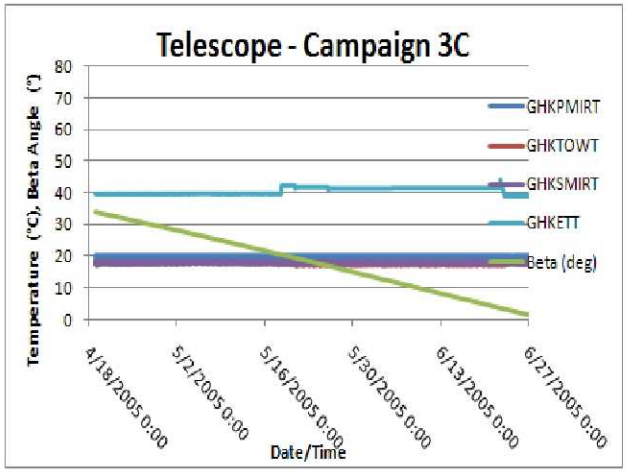

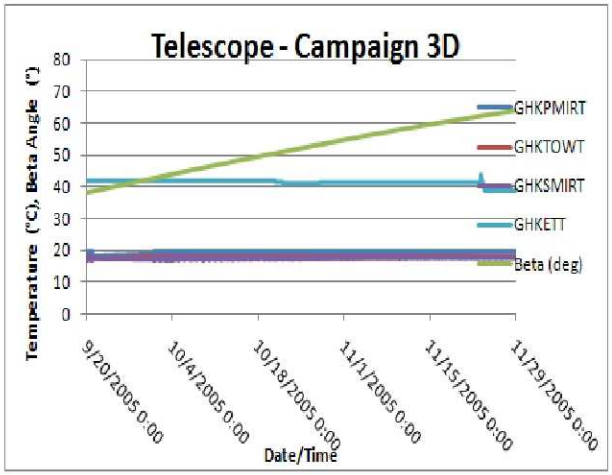

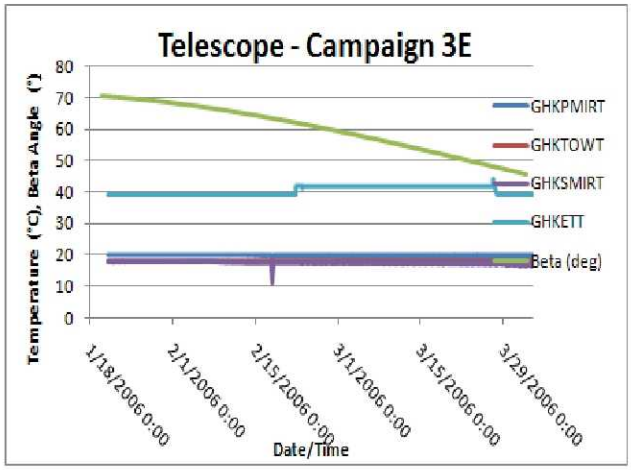

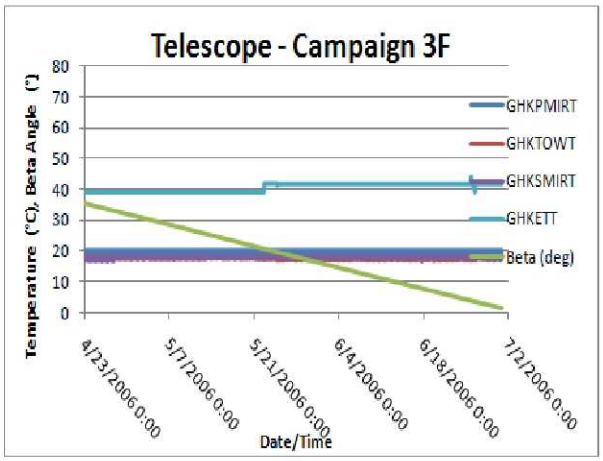

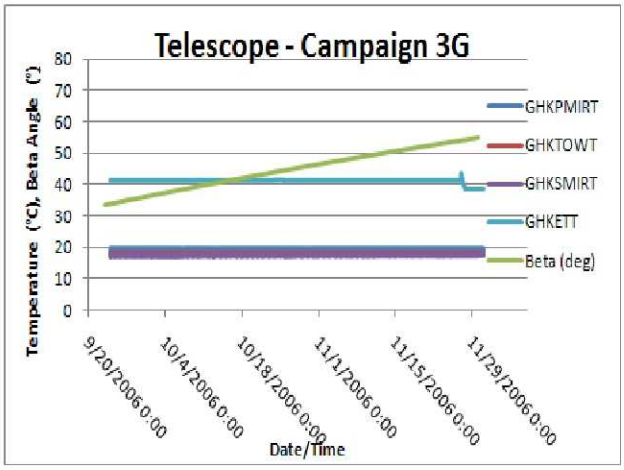

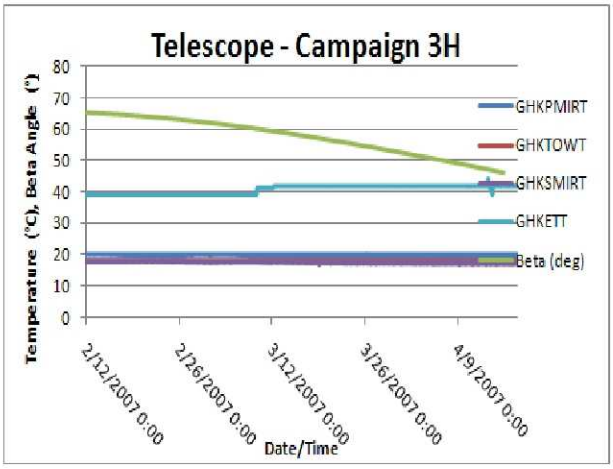

Appendix 5 - Telescope Telemetry (continued)